



# Orbital Debris

## Quarterly News

Volume 25, Issue 1  
February 2021

### Inside...

Characterization of the Eugene Stansbery-Meter Class Autonomous Telescope for GEO Survey Operations ..... 2

MMOD Inspection Results of ISS Battery Charge-Discharge Units ..... 4

Workshop Reports ..... 7

Upcoming Meetings ..... 8

2020 Breakup Events ..... 9

Monthly Object Type Charts by Number and Mass ..... 10

Space Missions and Satellite Box Score ..... 12

## Orbital Debris in the Latest U.S. National Space Policy

The topic of orbital debris was included in the U.S. National Space Policy for the first time in 1988. Under the “Inter-Sector Policies Section,” the policy states:

*“The directive further states that all space sectors will seek to minimize the creation of space debris. Design and operations of space tests, experiments and systems will strive to minimize or reduce accumulation of space debris consistent with mission requirements and cost effectiveness.”*

Every U.S. National Space Policy since that time has followed the same intent to focus on limiting the generation of new debris, with a somewhat expanded scope over time. For example, the 2010 U.S. National Space Policy also recognized the need to pursue research and development of technologies and techniques to mitigate and remove on-orbit debris (ODQN, vol.14, issue 3, p.1). The new U.S. National Space Policy, released in December 2020, continued that tradition with the following section on “Preserving the Space Environment to Enhance the Long-term Sustainability of Space Activities.”

**Preserve the Space Environment.** *To preserve the space environment for responsible, peaceful, and safe use, and with a focus on minimizing space debris the United States shall:*

- *Continue leading the development and adoption of international and industry standards and policies, such as the Guidelines for the Long-term Sustainability of Outer Space Activities and the Space Debris Mitigation Guidelines of the United Nations Committee on the Peaceful Uses of Outer Space;*

- *Continue to make available basic space situational awareness (SSA) data, and provide for basic space traffic coordination (including conjunction and reentry notifications), free of direct user fees while supporting new opportunities for United States commercial and non-profit products and services;*

- *Develop, maintain, and use SSA information from commercial, civil, and national security sources in an open architecture data repository to detect, identify, and attribute actions in space that are inconsistent with the safety, stability, security, and the long-term sustainability of space activities;*

- *Develop and maintain space flight safety standards and best practices to coordinate space traffic;*

- *Ensure that, consistent with international obligations, timely and accurate information concerning United States space objects launched into Earth orbit or beyond is entered into the United States domestic space object registry maintained by the Secretary of State and internationally registered with the United Nations as soon as practicable;*

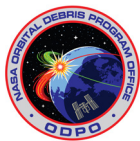
- *Limit the creation of new debris, consistent with mission requirements and cost effectiveness, during the procurement and operation of spacecraft, launch services, and conduct of tests and experiments in space by following and periodically updating the United States Government Orbital Debris Mitigation Standard Practices;*

- *Regularly assess existing guidelines for non-government activities in or beyond Earth orbit, and maintain a timely and responsive regulatory environment for licensing those activities, consistent with United States law and international obligations;*

- *Pursue research and development of technologies and techniques to characterize and to mitigate risks from orbital debris, reduce hazards, and increase understanding of the current and future debris environment;*

- *Evaluate and pursue, in coordination with allies and partners, active debris removal as a potential long-term approach to ensure the safety of flight in key orbital regimes;*

- *Require approval of exceptions to the United States Government Orbital Debris Mitigation Standard Practices from the head of the sponsoring agency and notification to the Secretary of State; and*



A publication of the  
NASA Orbital Debris  
Program Office (ODPO)

continued on page 2

## NSP

continued from page 1

• Continue to foster the development of best practices to prevent on-orbit collisions by collaborating with the commercial space sector and likeminded nations to: maintain and improve space object databases; pursue common international data standards and integrity measures; provide services

and disseminate orbital tracking information, including predictions of space-object conjunctions, to commercial and international entities; and expand SSA to deep space. ♦

## PROJECT REVIEW

# Characterization of the Eugene Stansbery-Meter Class Autonomous Telescope for GEO Survey Operations

C. CRUZ, B. BUCKALEW, S. LEDERER, AND T. KENNEDY

The goal in 2021 for the Eugene Stansbery Meter Class Autonomous Telescope (ES-MCAT) is to reach Full Operational Capability (FOC). This is defined by the proven capability to safely collect and autonomously process geosynchronous Earth orbit (GEO) survey data with calculated uncertainties, and by the ability to transmit results from its location on Ascension Island to the NASA Orbital Debris Program Office (ODPO) at Johnson Space Center in Houston, Texas. This data will be used to help build the populations for the next generation of the NASA Orbital Debris Engineering Model (ORDEM). To reach this capability, several tasks need to be completed, including verification and validation of the Observatory Control Software (OCS), safe and autonomous GEO observations, and securing a forward path to produce data for ORDEM through the use of the Orbital Debris Processing (ODP) software. One important task for FOC is to develop an autonomous GEO operations survey methodology to focus on the GEO orbital regime most likely to target orbital debris populations. This GEO survey method, characterizing the limiting magnitude and uncertainties, and the expected completeness of ES-MCAT data is discussed in this Project Review.

### GEO Survey Method

To generate populations for ORDEM, it was determined that the observation plan should result in sufficient observations so that every

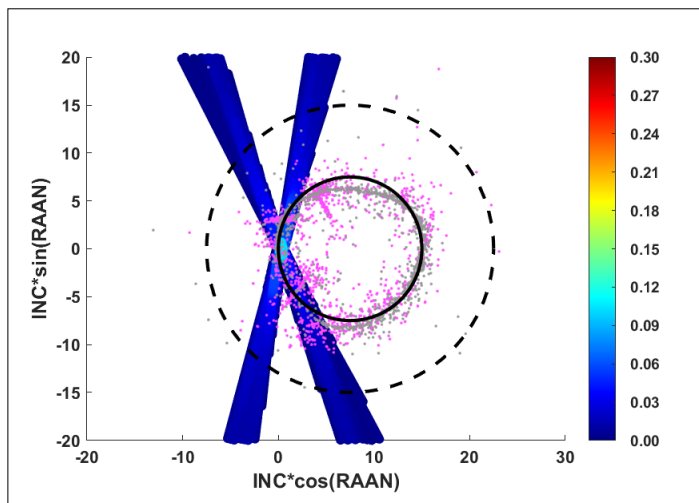


Figure 1. Tie-Dye plot showing the region of interest with the outer dashed circle, an inner circle corresponding with ORDEM GEO population data, a single night of data creating an "X" shape with an EVAL color bar, and a max EVAL of 0.106.

possible orbit in the designated orbital regimes targeted would have an expectation value (EVAL) of 0.3 or greater. The EVAL is used to assign each object a weight, representing the number of times that target should be counted when building populations for ORDEM. This weighting statistically accounts for multiple detections of the same object, as well as detections of objects that are samples from a larger population that is, on average, undetected or under-sampled. With a complete GEO survey, every possible GEO object (bright enough to be detected) in orbits with inclination (INC) and right ascension of ascending node (RAAN) in the region of interest would have a 0.3 or higher probability of being detected sometime during the observation campaign (assuming randomized mean anomaly). This region of interest is defined (see ODQN vol. 24, issue 2, April 2020, p. 4) as an annular area in the Cartesian coordinates of  $(INC \cdot \cos(RAAN), INC \cdot \sin(RAAN))$  centered at  $(7.5^\circ, 0^\circ)$  with a radius of  $15^\circ$ , as shown by the dashed outer circle in Figure 1. The gray and pink dots represent the modeled GEO intact objects and fragmentation debris, respectively, used to develop the ORDEM 3.1 model.

An ODPO prediction and probability coverage software, known as "Tie-Dye" (derived from the colorful plots produced), calculates EVALs for given INC and RAAN pairs using observation parameters such as the right ascension (RA), declination (Dec), and the date/time of each observation frame as inputs. These parameters define a field center vector, which is then compared to the vectors of artificial objects' orbits with varying RAANs, INCs, and mean anomalies. The orbits are assumed to be geosynchronous, with semi-major axes of 42,164 kilometers, and eccentricities of 0. For a given INC/RAAN pair, the program sweeps through 1,000 values of starting mean anomaly to see what fraction of such objects could have been observed by the telescope in each frame. If the telescope could have observed the given orbit for four frames, then it is registered as a "detect." The fraction of such "detects" from the list of possible starting mean anomalies defines the EVAL for that INC/RAAN orbit for that night of observation.

To minimize oversampled regimes and focus on undersampled regions in the GEO zone with ES-MCAT, a survey strategy is necessary. This strategy will determine where to point the telescope optimally in RA and Dec space at different hours for different times of the year.

The creation of this strategy is partly achieved by the Tie-Dye program, used in a previous survey of the GEO orbital regime [1]. Different observation strategies can be tested using the Tie-Dye program. By planning a set of RA/Dec observation windows during a night, it is possible to create a two-dimensional map of EVALs in INC/RAAN space. In general, during an observational night, two RAs are observed: one hour (or 15 degrees) before and one hour after the RA of Earth's shadow. This strategy assures that the observations stay near Earth's shadow, and

continued on page 3

# ES-MCAT FOC

continued from page 2

thus maximize the backscatter brightness of the object. Each of these RAs are observed in two halves of the night, with the switch usually occurring in the early morning. To concentrate observations in Figure 1's annulus and increase the coverage of higher inclinations, the following survey approach was developed. Named the "Candy Cane" survey approach, due to its appearance, it follows the shape of the GEO belt and ensures uniform coverage throughout the INC/RAAN region of interest. Cycles of 25 nights of observations are completed that cover a portion of the GEO belt in RA/Dec space, shown in Figure 2. These cycles are continued until the region of interest in INC/RAAN space is sufficiently covered. By following Earth's shadow, the RA is increased each night by approximately 4 minutes (1 degree). This process creates two diagonal columns in RA/Dec space on the GEO belt. After 14 cycles (350 nights), the field centers span the entirety of RA space in the GEO belt, as shown in Figure 3.

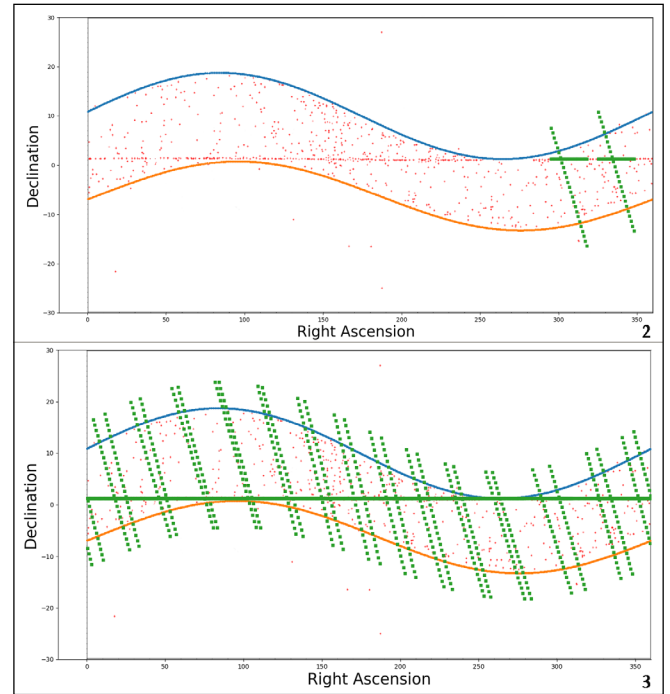
Using this approach, predicted field centers were created. To simulate actual weather down-time and non-photometric nights, subsets of observing days were removed from predicted field centers based on a 2005–2009 historical cloud model for Ascension Island, thus creating monthly availability percentages [2]. These modified field centers provided inputs for the Tie-Dye program, which produced predicted INCs and RAANs along with their corresponding EVALs.

The plot in Figure 4 encompasses a single 25-night cycle, where a single night's data creates an "X" swath shape, as in Figure 1. These X's begin on the bottom left of the dashed circle and continue to span the circle, while rotating slightly counterclockwise, until they reach the top of this outer circle. The X's are also created at (0°, 0°) where the section of the GEO belt with approximately 0° Dec is continuously observed. With this movement of coverage in the INC/RAAN space, and with the addition of more cycles, the region of interest can be covered with expectation values of 0.3 or greater while minimizing over-coverage. The Tie-Dye plot of 14 cycles/350 nights is shown in Figure 5. As the survey progresses, the region of interest, for actual observations, will be monitored and temporary adjustments in observations may be made to fill in some spaces that were unobserved or under-observed due to weather or clouds.

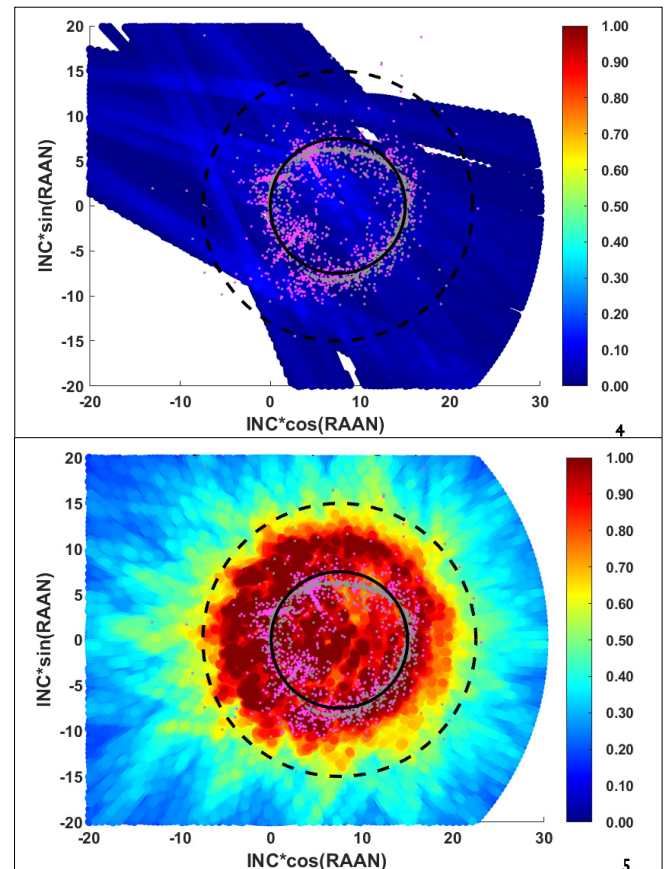
## Sidereal Tracking Limiting Magnitude

To determine the limiting magnitude of ES-MCAT, the dimmest detected magnitude in every sidereal tracked (ST) image taken with a Sloan Digital Sky Survey r' filter, used for calibration and system monitoring, was extracted. These data span 53 nights between the dates of 16 April 2020 and 10 August 2020 and are plotted in Figure 6 versus the infrared extinction (as measured on site using a FLIR Systems infrared camera, and hereafter "FLIR extinction," etc.). A FLIR value of 0.00 indicates clear, photometric skies (i.e., no clouds at all), and a maximum extinction value of 4.00 was utilized. The FLIR value plotted for each point is the average of the FLIR value observations taken before and after the image, and not the true continuous FLIR average precisely overlapping the 10-second exposure time – this causes scatter in the data.

Throughout the range of FLIR values from 0 to 4, the dimmest magnitudes do not appear to exceed a value of approximately 19.5 (indicated by the dashed line in Figure 6). For further investigation into this flat trend, the faintest magnitude data points were separated into sections incremented by 0.25. The faintest magnitude value was then computed for each set, which were then averaged together. This averaged value, along with its standard deviation, produces a limiting magnitude. Based on the current ES-MCAT configuration, condition of optical components, operations, and data processing, the limiting magnitude to 1σ is 19.48 ± 0.18.



Figures 2 (top) and 3 (bottom). GEO belt in RA/Dec space with overlay of predicted field centers using "Candy Cane" Method for 25 (1 cycle) and 350 (14 cycles) nights, respectively.



Figures 4 (top) and 5 (bottom). Tie-Dye plots utilizing predicted field centers from "Candy Cane" Method for 25 and 350 nights, respectively. Note that the Tie-Dye program creates artificial orbits with a maximum INC of 30° for this analysis.

continued on page 4

## ES-MCAT FOC

continued from page 3

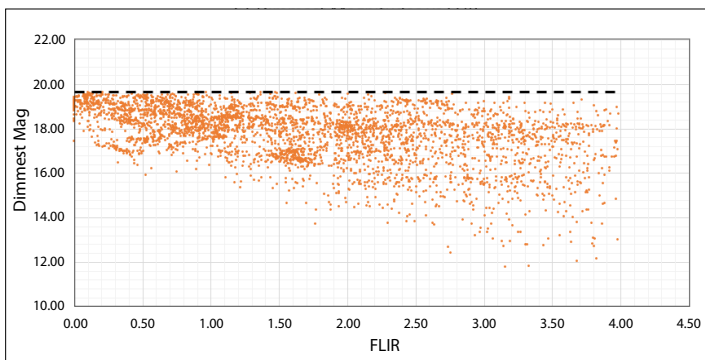


Figure 6. ST images indicate the dimmest magnitudes detected in each image versus FLIR extinction. A FLIR value of 0.00 indicates clear, photometric skies (i.e., no clouds at all) and the FLIR value indicates (roughly) the average extinction (in magnitudes) observed by the FLIR infrared camera over a 10° field of view. The dimmest magnitude depends on the faintest object in that field of view, which will be predominantly affected by the atmospheric extinction between the telescope and each star.

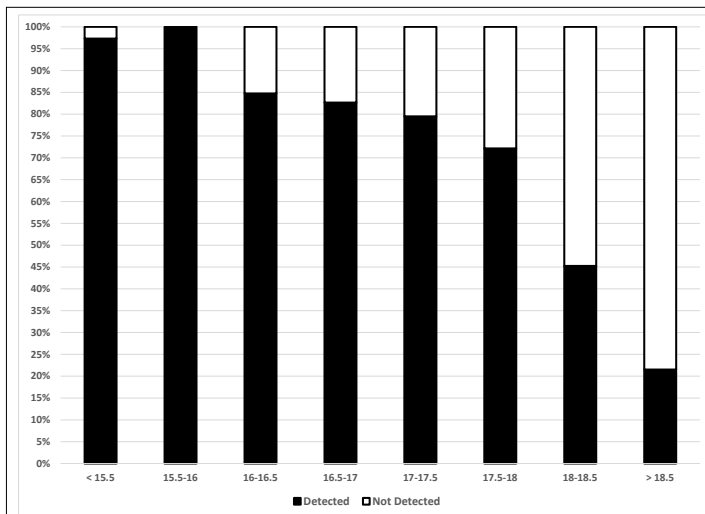


Figure 7. Relative completeness of detections as a function of magnitude. Bins are labeled with their range. Solid black is the percentage of point sources detected by OCS. Solid white is the percentage of point sources not detected by OCS.

### Rate Tracked Magnitude Completeness

Completeness indicates how well a telescope system can detect a point source of a specific magnitude. OCS completeness values are simulated over the magnitudes detected by ES-MCAT utilizing rate tracked (RT) GEO survey data acquired on 22 June 2020. From the OCS field center file, image sets were randomly chosen for the insertion of artificial point sources. These point sources were placed in each set of images with the same magnitude and pixel position; instrumental magnitudes ranged from -10.5 to -8.5 in increments of 0.5. Note the instrumental magnitude provides the uncalibrated apparent magnitude of these simulated point sources.

After OCS processed the modified images, the object detect files were manually analyzed to determine whether the system detected the artificial point sources. The successful and failed group results were binned and are presented in relative percentages in Figure 7. Note that there are uncertainties in these completeness percentages due to multiple factors including the binning method, OCS's processing uncertainties, and variations in the images themselves. The limiting magnitude of the system dictates where the detection threshold goes to 0%. While stochastic detections of point sources dimmer than 19.5 are still possible, their use for building ORDEM populations would be limited.

### Summary and Path Forward

The calculation of the limiting magnitude of ST images for the optical components that will be utilized during the GEO survey and the characterization of the system's ability to detect objects in RT images helps in understanding the capabilities of ES-MCAT for use in developing the GEO survey. With the determination of an optimal survey strategy that both minimizes oversampled regimes and focuses on the region of interest, ES-MCAT can continue its path towards FOC and beyond by gathering observational data for building debris populations in ORDEM.

### References

1. Abercromby, K.J., Seitzer, P., *et al.*, A Summary of Five Years of Michigan Orbital Debris Survey Telescope (MODEST) Data, 59th International Astronautical Congress, 2008.
2. Lederer, S.M., Cruz, C.L., *et al.*, NASA's Orbital Debris Optical Program: ES-MCAT Nearing Full Operational Capability (FOC), AMOSTechnical Conference Proceedings, 2020. ♦

## PROJECT REVIEW

### MMOD Inspection Results of ISS Battery Charge-Discharge Units

J. HYDE, E. CHRISTIANSEN, AND D. LEAR

The Battery Charge-Discharge Unit (BCDU) is a component in the International Space Station (ISS) electrical power system. There are 24 BCDU boxes on the ISS, with three units located in the truss at the base of each solar array (Figure 1). The BCDU enclosure is 102.7 cm long, 73.2 cm wide, and 30.3 cm tall. The enclosure cover is a sandwich

panel construction with thin aluminum facesheets and a single layer of betacloth bonded to the outer facesheet. The impacted surfaces involved in the inspections described below did not have a constant attitude relative to the ISS body axes. The outboard ISS truss segments that house each BCDU are designed to track the sun to aid in solar array pointing. During nominal operations, the truss segments perform one revolution during a 90-minute ISS orbit.

continued on page 5

# BCDU MMOD RESULTS

continued from page 4

Table 1. BCDU Exposure Details

BCDU	LOCATION	EXPOSURE START	DEPLOYED	EXPOSURE END	RETURNED	EXPOSURE
SN: 0016	P4, 4A3	GMT 253/2006	STS-115 (12A)	GMT 135/2019	SpX-17	12.68 years
SN: 0011	P6, 2B2	GMT 336/2000	STS-97(4A)	GMT 291/2019	SpX-19	18.88 years

Figure 1 illustrates the location of BCDU-0016 on ISS truss segment P4 and BCDU-0011 on P6. Both units failed on orbit in 2019 and were subsequently removed and replaced by extravehicular activity. The failed BCDUs were returned to the ground for repair on a Cargo Dragon spacecraft. The failures were not related to micrometeoroid and orbital debris (MMOD) impacts; however, inspections were performed of both units to determine the number and size of damages on the exterior surfaces of the BCDU that were caused by MMOD. Table 1 provides details on the two inspected BCDUs. Serial number (SN) 0016 came back with nearly 13 years of exposure time and SN 0011 accumulated almost 19 years of exposure time.

Both BCDUs were inspected for impact features that resulted in at least one betacloth fiber bundle completely severed. This equated to feature diameters greater than about 300 microns. A typical impact feature can be seen in Figure 2. At this level of magnification, the individual fiberglass strands in the betacloth weave can easily be discerned. This distinctive grouping of severed fiber bundles was the general criteria used by the inspection team to designate hypervelocity impact damage in the surface areas of the BCDU covers. This same type of damage has been reproduced in a recent hypervelocity impact test campaign of similar materials (Figure 3). Figure 2 also illustrates the general protocol used to record damage size measurements in the betacloth. If damage was observed in the underlying aluminum facesheet, crater dimensions were also recorded. The inspection team also observed a small number of impact craters in areas of anodized aluminum regions. Dimensions for craters in aluminum were obtained in the plane of the original facesheet. If the facesheet was perforated, an exit hole dimension also was obtained. There were also a handful of impact sites on the coated aluminum. In these cases, the aluminum crater diameter was measured as well as the diameter of the coating spall zone.

The July 2019 inspection of BCDU-0016 yielded 63 MMOD impact features. Most of the impact features were located on the cover since it faced outward from the truss and was not blocked from impacts by adjacent hardware. Fifty-one MMOD indications were recorded on the cover. The enclosure sides were available for inspection, but they yielded a smaller number (12) of MMOD indications. The smaller number was expected due to the BCDU's proximity to other equipment (Figure 1).

In February 2020, an inspection was performed on the cover of BCDU-0011. As with the previous effort, most impact features were located on the cover where 27 regions of interest were recorded. Four additional impact features were observed on the sides, which were difficult to access for inspection due to the presence of the BCDU shipping container walls. The MMOD inspection of BCDU-0011 was highlighted by two impacts on the cover that induced perforations in the aluminum facesheet. The left-hand image in Figure 4 shows impact feature #1 as initially observed, while the right-hand image illustrates the effect

of slightly moving the severed betacloth fibers away from the facesheet damage area. This action was necessary to allow the measurement of the crater in the aluminum and was accomplished with a bamboo probe. The betacloth damage diameter measured 1.16 mm. The facesheet crater diameter was measured at 0.66 mm and the exit hole at the crater bottom was 0.27 mm. The largest impact feature observed on BCDU-0011 (#2) occurred on the opposite end from impact #1 on the edge of the cover adjacent to a painted closeout edge. This impact site did not require the betacloth manipulation needed at impact #1 to measure the damage sizes in the aluminum. Damage diameter in the betacloth was 1.70 mm, the aluminum crater diameter measured 0.72 mm and the exit hole diameter

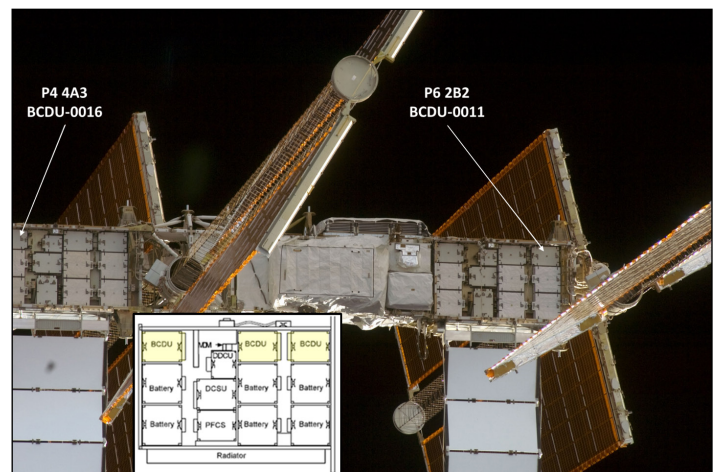


Figure 1. BCDU-0016 location on P4 and BCDU-0011 location on P6. Inset: bottom view of the Integrated Equipment Assembly, each of which houses three BCDUs.

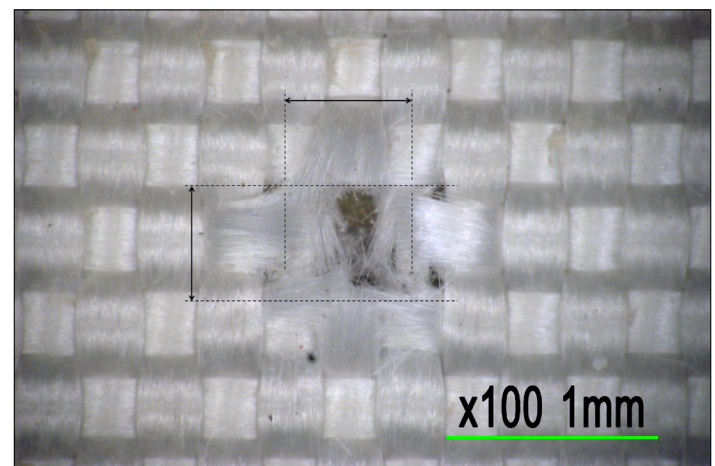


Figure 2. Typical impact feature in BCDU, with entry hole measurements illustrated.

continued on page 6

# BCDU MMOD RESULTS

continued from page 5

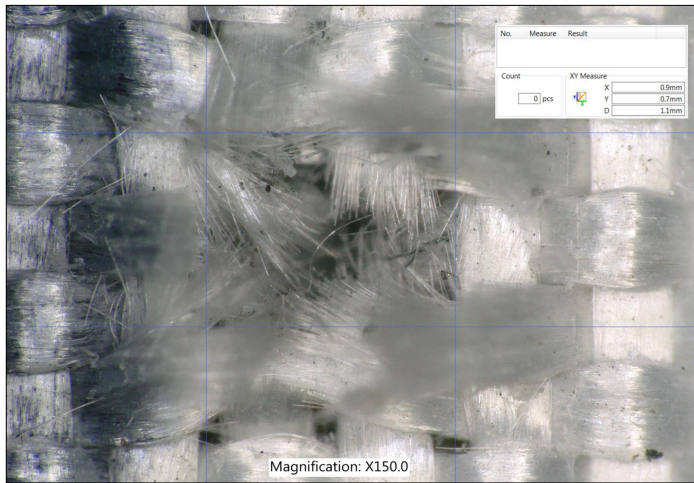


Figure 3. Results from test HITF19279, 200-micron diameter Al2017-T4 projectile at 0 degrees and 7 km/s.

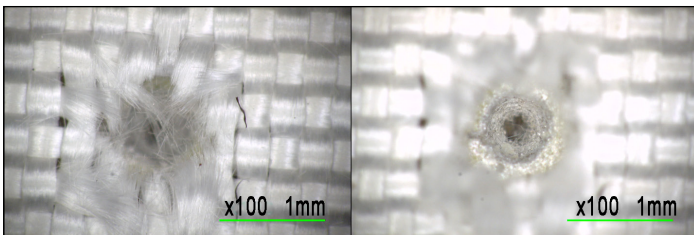


Figure 4. BCDU-0011 impact #1, before and after betacloth manipulation.

Table 2. BCDU Inspection Summary

BCDU	TOTAL # OF IMPACTS	# OF IMPACTS - COVER	# OF IMPACTS - SIDES	# OF FACESHEET PERFORATIONS	# OF IMPACTS - BETACLOTH	# OF IMPACTS - AI	AVER FEATURE DIAMETER (MM)	MAXIMUM FEATURE DIAMETER (MM)
SN: 0016	63	51	12	0	44	19	0.38	0.81
SN: 0011	31	27	4	2	25	6	0.64	1.7

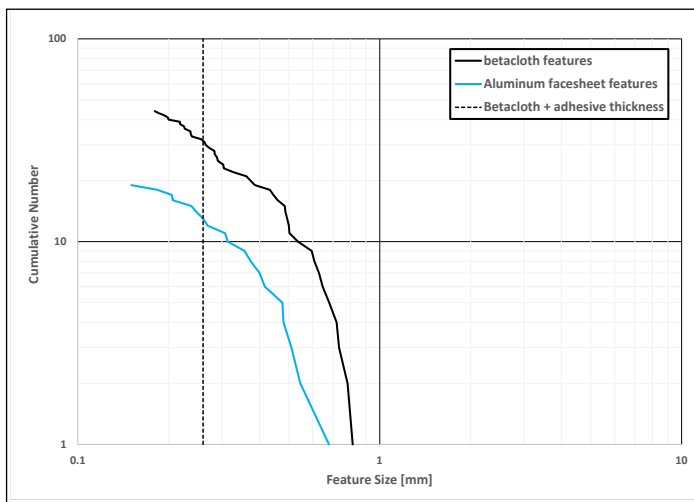


Figure 5. BCDU-0016 cumulative number as a function of feature size. A total of 44 impact features were observed in the Betacloth blanket, the holes ranging from 0.18 mm to 0.81 mm in diameter. Nineteen additional craters in the aluminum facesheet or anodized fixtures were noted; these ranged from 0.15 mm to 0.68 mm in diameter. See also Table 2.

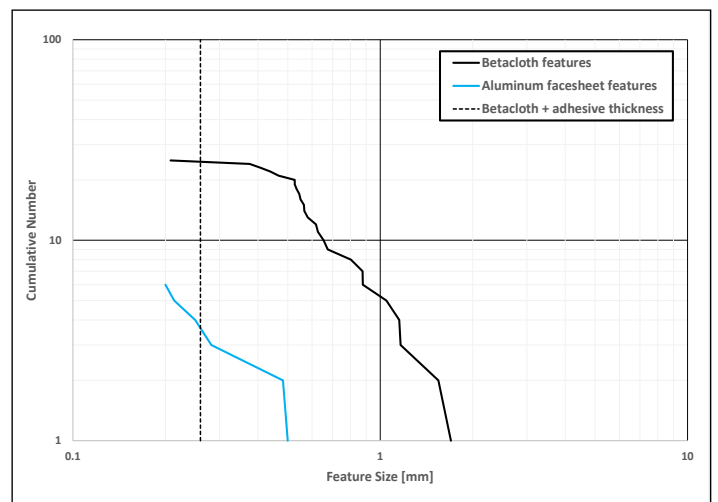


Figure 6. BCDU-0011 cumulative number as a function of feature size. This panel's features included Betacloth blanket holes (25 observations ranging from 0.21 mm to 1.70 mm in diameter) and damage to the aluminum facesheet or anodized fixtures (six craters ranging from 0.20 mm to 0.50 mm in diameter). See also Table 2.

was 0.38 mm. The cover was still attached to the BCDU-0011 enclosure, so inspection of the inner facesheet surface for damage was not possible. Due to the flight hardware classification of both sets of hardware, the inspection team was not permitted to request intact extraction of samples for laboratory analysis of impactor residues.

In March 2020, a re-inspection of BCDU-0016 was performed to investigate the possibility that the initial inspection may have missed threshold facesheet perforations due to the obscuring effect of the betacloth fibers. Fourteen of the largest impact sites on the cover were manipulated with a bamboo probe to expose the underlying facesheet damage. None of the 14 investigation sites exhibited clear evidence of a facesheet perforation. Facesheet crater diameter data was recorded for the newly exposed sites and added to the impact database.

Figure 5 and Figure 6 show the distribution of impact feature sizes for BCDU-0016 and -0011, respectively. Distributions are provided for aluminum crater diameter and betacloth damage diameter. Table 2 summarizes measurement statistics.

Future work involves comparing the observed number of damage features in the betacloth and aluminum with Bumper code predictions of damage sizes using the ORDEM 3.1 orbital debris and MEM 3 meteoroid environments. The as-flown assessment will incorporate the yearly average ISS altitude for each flight year from 2000 to 2019 as well as the orientation and shadowing effects of the outboard truss rotations required for solar array pointing. ♦

# WORKSHOP REPORTS

## NASA Aerospace Battery Workshop, 17-19 November 2020, Huntsville, AL, USA (Virtual)

The NASA Aerospace Battery Workshop was conducted virtually from 17 to 19 November 2020. This annual workshop is hosted by Marshall Space Flight Center and sponsored by the NASA Engineering and Safety Center. The global battery engineering community was represented by over 300 participants from academia, industry, and government. The live, virtual format allowed for a larger attendance, maintained the live question-and-answer periods, and allowed the organizers to schedule additional presentations in lieu of breaks.

This year's workshop included 40 presentations covering topics such as cell assembly and testing hardware, test instruments, performance modeling and prediction, several aspects of thermal runaway, solid-state batteries and other new lithium-ion (Li-ion) chemistries, and the state of the industry. Although the focus of this workshop typically does not extend to orbital debris policy issues, with the increased use of common Li-ion cells in spacecraft design the NASA Orbital Debris Program Office presented "NASA Orbital Debris Mitigation Requirements Applied to Batteries". The presentation included an overview of debris mitigation policy and NASA requirements, and discussed the compliance challenges

faced by space mission designers. The goal of presenting to this audience was to raise awareness of battery explosion and passivation issues, as applied to orbital debris mitigation, among members of the battery research, development, and production community.

Of the many interesting and informative presentations, a sampling of those related to debris mitigation included: cell materials that tolerate internal shorts; a battery housing that protects cells from damage and the battery from individual cell failures; how state-of-charge affects onset and outcome of thermal runaway; efforts to control cell fragments during thermal runaway; and the development of an active, liquid-cooled battery matrix design, demonstrated to be capable of dissipating the energy equivalent to the thermal runaway of a single cell.

The NASA Aerospace Battery Workshop continues to provide a valuable opportunity for representatives from industry, academia, and government to assemble and discuss modeling capabilities, the state of battery design and performance, and future trends and expectations. Presentations from this and past workshops are available at <https://www.nasa.gov/batteryworkshop>. ♦

## 5th International Space Debris Reentry Workshop, 2 December 2020, Darmstadt, Germany (Virtual)

The 5th International Space Debris Reentry Workshop was hosted by the European Space Agency's Space Operations Centre in Darmstadt, Germany, and is conducted on an aperiodic basis whenever an important problem or concern is raised within the orbital debris community. The workshop was conducted in a virtual format, allowing increased participation by several hundred participants across the European Union and United States.

This year, the workshop focused on the challenges of reentry breakup modeling and prediction, with 19 presentations covering probabilistic reentry breakup models, upper atmosphere dynamics, demise of composite materials, and in-situ reentry experiments. The workshop was broken into five sequential panel discussions on materials, aerothermodynamics, break-up simulations, orbital predictions and observations, and missions.

The NASA Orbital Debris Program Office presented recent work on adapting the Object Reentry Survival Analysis Tool (ORSAT) to run Monte-Carlo type object reentry simulations, and the results

from preliminary simulations of a hypothetical spacecraft that show to what degree second-order effects like atmospheric thermal expansion and contraction have on the debris casualty area of a spacecraft. The European Space Agency has incorporated various European reentry risk modeling codes into a probabilistic assessment model, which provided a good opportunity for exchange in the session discussion.

It is worth noting that all the presentations in the "Materials" panel session focused on the need to better understand the demise of carbon composite components, particularly composite overwrapped pressure vessels. With the increase in the use of these materials in modern spacecraft, there is a growing realization within the community that our current understanding of the reentry demisability of these materials is insufficient.

Proceedings of the workshop, including PDF versions of the presentations, can be found at <https://conference.sdo.esoc.esa.int/proceedings/list?search=&conference=10>. ♦

## DAS 3.1 NOTICE

Attention DAS Users: DAS 3.1 has been updated to DAS 3.1.1. Previous versions of DAS should no longer be used. NASA regulations require that a Software Usage Agreement must be obtained to acquire DAS 3.1.1. DAS 3.1.1 requires the Windows operating system and has been extensively tested in Windows 10.

To begin the process, click on the Request Now! button in the NASA Software Catalog at <https://software.nasa.gov/software/MSO-26690-1>. Users who have already completed the software request process for earlier versions of DAS 3.x do not need to reapply for DAS 3.1.1. Simply go to your existing account on the NASA Software portal and download the latest installer.

An [updated solar flux table](#) (created 16 December 2020) can be downloaded for use with DAS 3.1.1.

## UPCOMING MEETINGS

These events could be canceled or rescheduled due to the COVID-19 pandemic. All information is current at the time of publication. Please consult the respective websites for updated schedule changes.

### 2–4 March 2021: **Virtual 1st MASTER Workshop 2021**

The Meteoroid and Space Debris Terrestrial Environment Reference (MASTER) model has been developed by the European Space Agency. This virtual workshop intends to initiate the discussion on how collaborative approaches can be established to facilitate exchange of data and measurement collection (including ground-based measurements, in-situ detectors, returned surfaces, and novel measurements), its interpretation and application in the MASTER modelling context, the use-cases of the model, and its relevance in mission design. Additional information about this conference is available at <https://indico.esa.int/event/370/>.

### 20–23 April 2021: **Virtual 8th European Conference on Space Debris**

The European Space Agency's European Space Operations Center, Darmstadt, Germany, will host the 8th European Conference on Space Debris in virtual format. This quadrennial event will address all fundamental, technical areas relevant to the orbital debris community, including measurement techniques, environment modelling theories, risk analysis techniques, protection designs, mitigation and remediation concepts, and standardization, policy, regulation & legal issues. The deadline for abstract submission has passed. Additional information about this conference is available at <https://space-debris-conference.sdo.esoc.esa.int/>.

### 7–12 August 2021: **35th Annual Small Satellite Conference, Logan, UT, USA**

Utah State University (USU) and the AIAA will sponsor the 35th Annual AIAA/USU Conference on Small Satellites, whose theme is “Mission Operations and Autonomy: operations and data delivery at the speed of light,” and will explore the realm of new space mission operations and autonomy enablers. The abstract submission deadline has passed. Conference information is available at the organizer's website at <https://smallsat.org/>. Attendance options (virtual vs. in-person) have not been determined at this time.

### 13–15 September 2021: **3rd IAA Conference on Space Situational Awareness, Madrid, Spain**

The International Academy of Astronautics (IAA) and the University of Florida will convene the 3rd IAA Conference on Space Situational Awareness in September 2021; the University of Florida will provide a remote participation option should the COVID-19 pandemic not be resolved by meeting time. Topics include, but are not limited to, resident space object sensing; identification, association, and risk assessment; remediation and reentry; and policy. Abstract submission closes on 15 June 2021. Please see <https://iaaspace.org/event/3rd-iaa-conference-on-space-situational-awareness-icssa-2021/> or <http://reg.conferences.dce.ufl.edu/ICSSA/1575> for further information.

### 14–17 September 2021: **22nd Advanced Maui Optical and Space Surveillance Technologies Conference, Maui, Hawaii, USA**

The technical program of the 22nd Advanced Maui Optical and Space Surveillance Technologies Conference (AMOS) will focus on subjects that are mission critical to Space Situational Awareness/Space Domain Awareness. The technical sessions include papers and posters on Orbital Debris, Space Situational/Space Domain Awareness, Adaptive Optics & Imaging, Astrodynamics, Non-resolved Object Characterization, and related topics. The abstract submission deadline is 1 March 2021. Additional information about the conference is available at <https://amostech.com>.

### 25–29 October 2021: **72nd International Astronautical Congress (IAC), Dubai, United Arab Emirates**

The IAC will convene with a theme of “Inspire, Innovate & Discover, for the Benefit of Humankind.” The IAC's 19th IAA Symposium on Space Debris shall cover debris measurements, modeling, risk assessment including re-entry hazards, mitigation and remediation, hypervelocity impact and protection, political and legal aspects of space debris mitigation and removal, and allied subjects. Abstract submission closed on 28 February 2020. Additional information for the 2021 IAC is available at <https://www.iaastro.org/events/iac/iac-2021/> and <http://iac2021.org/>.

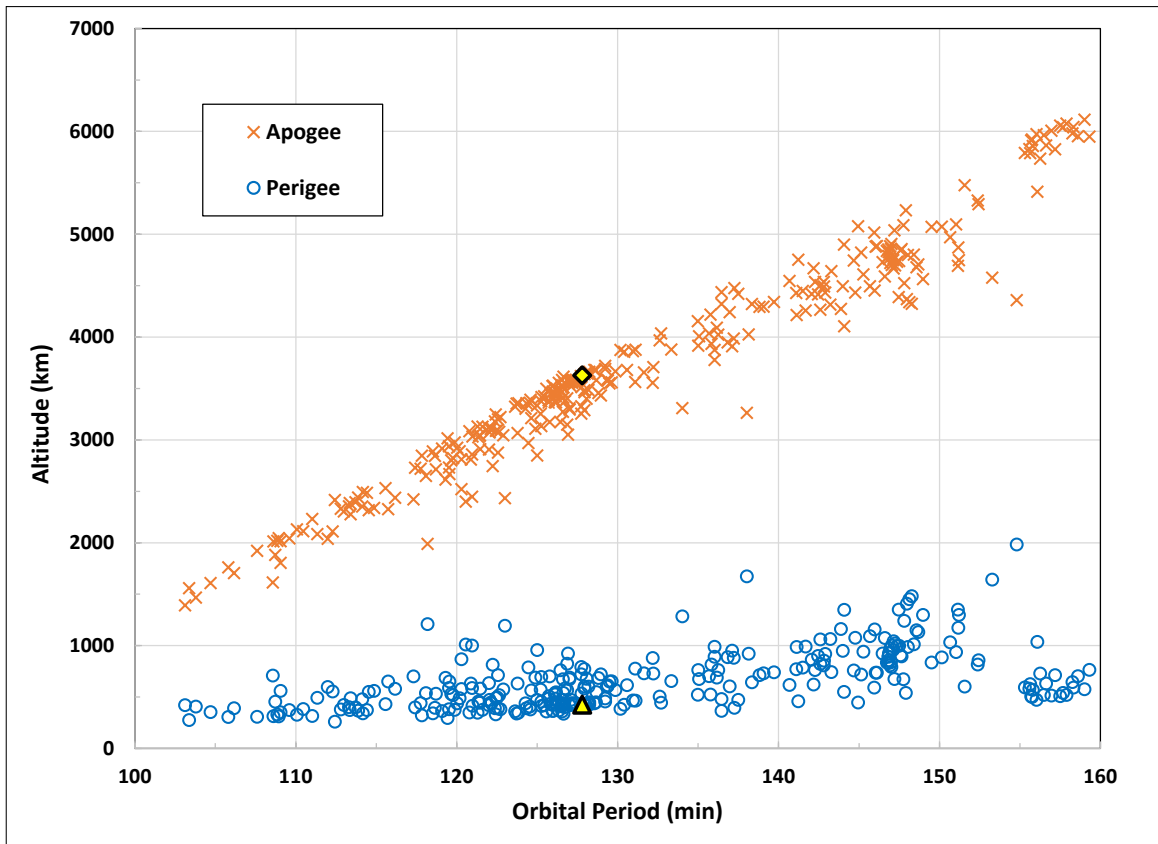
# BREAKUP EVENTS IN 2020

BREAKUP DATE	SATELLITE NAME	INTERNATIONAL DESIGNATOR	PERIGEE ALT (KM)	APOGEE ALT (KM)	INCLINATION (DEG)	DEBRIS CATALOGED	DEBRIS LEFT
9 Jan. 2020	Cosmos 2535	2019-039A	604	618	97.9	26	13
12 Feb. 2020	SL-14 <i>Tsyklon</i> 3rd stage	1991-056B	1,186	1,206	82.6	112	108
8 May 2020	SL-23 <i>Zenit Fregat</i> tank	2011-037B	422	3,606	51.5	325	309
12 July 2020	H-2A fairing cover	2018-084C	595	643	97.9	87	28
27 Aug. 2020	<i>Resurs-O1</i> spacecraft	1994-074A	633	660	97.9	72	72

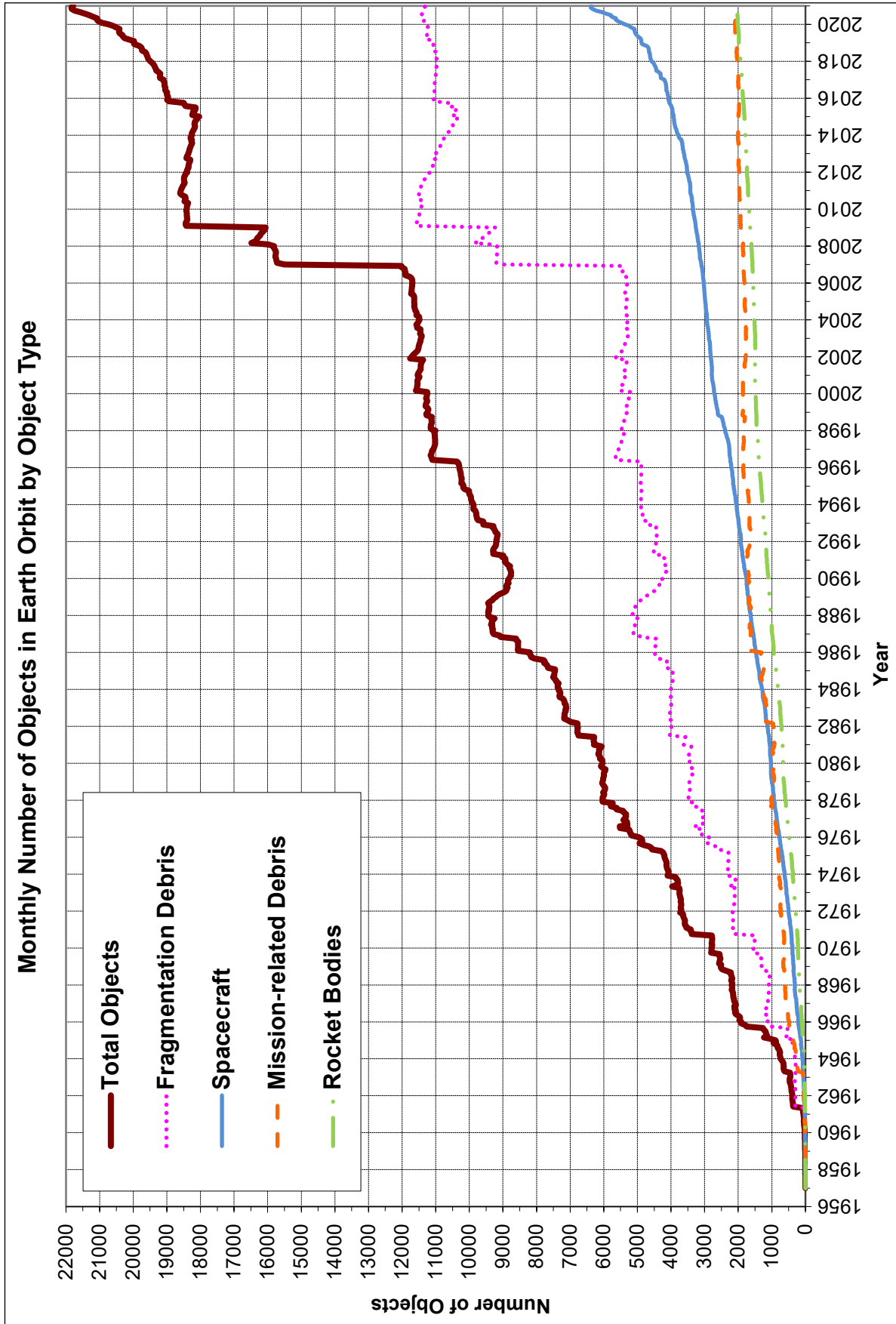
Five documented breakup events that occurred in 2020 are listed in the table above. The table lists the international designator, perigee altitude, apogee altitude, and inclination of each parent object at the time of the breakup. Fragment counts in the two far right columns are based on data provided by the Space Force's 18th Space Control Squadron as of 1 February 2021. These fragments are large enough to be tracked by the U.S. Space Command's Space Surveillance Network (SSN). Many more debris too small to be tracked/cataloged by the SSN but large enough to threaten human spaceflight and robotic missions were also generated from these breakup events. Orbital debris mission-ending risk to robotic spacecraft operating in low Earth orbit is actually driven by the small, untracked debris in the millimeter size regime.

The breakup of the SL-23 Zenith upper stage Fregat tank on 8

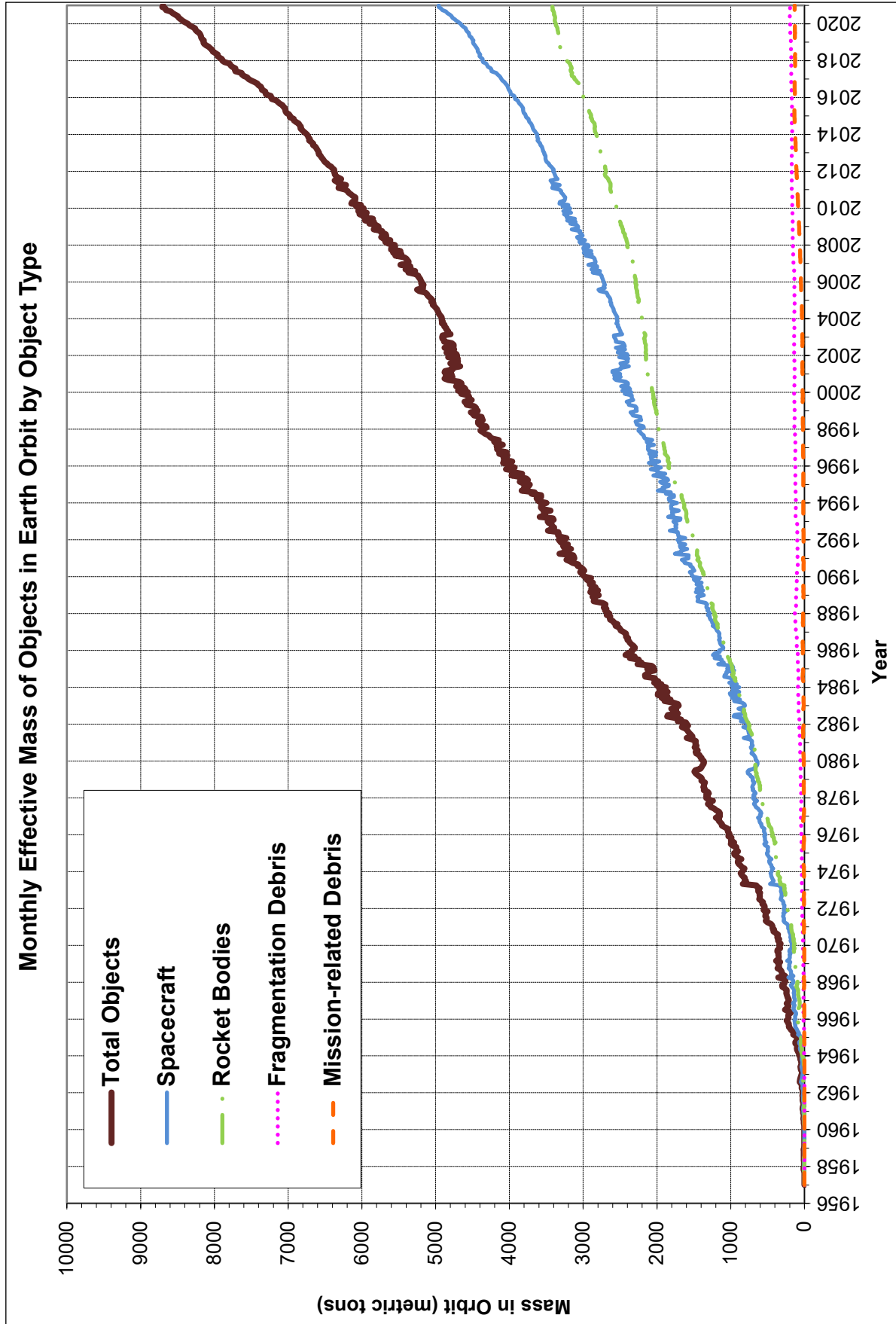
May 2020 was reported in the August 2020 Issue of the Orbital Debris Quarterly News (ODQN, Vol. 24, Issue 3, pp. 2-3). Additional fragments associated with the event have been identified and tracked by the SSN since that time. Based on the new data, this breakup has turned out to be the most severe fragmentation event over the past 5 years. As of 1 February 2021, a total of 325 fragments, including the parent object, were large enough to be tracked and cataloged by the SSN, and only a very small fraction (~5%) of them had decayed/reentered 10 months after the event. The Gabbard diagram below is based on the SSN data on February 1. The parent object is indicated by the diamond and triangle symbols. Because of the orbit of the parent object and the energetic nature of the breakup, the Fregat tank fragments spread over a wide range in altitude, from 100 km to 6,000 km and above. ♦



Gabbard diagram of the Fregat tank fragments based on the 1 February 2021 SSN data.



Monthly Number of Cataloged Objects in Earth Orbit by Object Type as of 5 January 2021. This chart displays a summary of all objects in Earth orbit officially cataloged by the U.S. Space Surveillance Network. "Fragmentation debris" includes satellite breakup debris and anomalous event debris, while "mission-related debris" includes all objects dispensed, separated, or released as part of the planned mission.



Monthly Mass of Objects in Earth Orbit by Object Type as of 5 January 2021. This chart displays the mass of all objects in Earth orbit officially cataloged by the U.S. Space Surveillance Network.

## SATELLITE BOX SCORE

(as of 05 January 2021, cataloged by the  
U.S. SPACE SURVEILLANCE NETWORK)

Country/ Organization	Spacecraft*	Spent Rocket Bodies & Other Cataloged Debris	Total
CHINA	441	3810	4251
CIS	1551	5696	7247
ESA	93	56	149
FRANCE	72	510	582
INDIA	101	119	220
JAPAN	189	145	334
USA	2866	4998	7864
OTHER	1131	123	1254
<b>TOTAL</b>	<b>6444</b>	<b>15457</b>	<b>21901</b>

\* active and defunct

Visit the NASA

Orbital Debris Program Office Website

[www.orbitaldebris.jsc.nasa.gov](http://www.orbitaldebris.jsc.nasa.gov)

**Technical Editor**

Phillip Anz-Meador, Ph.D.

**Managing Editor**

Rossina Miller

**Correspondence can be sent to:**

J.D. Harrington

[j.d.harrington@nasa.gov](mailto:j.d.harrington@nasa.gov)

**or to:**

Nilufar Ramji

[nilufar.ramji@nasa.gov](mailto:nilufar.ramji@nasa.gov)

## INTERNATIONAL SPACE MISSIONS

01 September – 30 November 2020

Intl.* Designator	Spacecraft	Country/ Organization	Perigee Alt. (KM)	Apogee Alt. (KM)	Incli. (DEG)	Addnl. SC	Earth Orbital R/B	Other Cat. Debris
1998-067	ISS dispensed CubeSats	USA	410	412	51.6	7	0	0
2020-061A	NUSAT-6 HYPATIA	ARGENTINA	495	507	97.4	62	0	0
2020-062A	STARLINK-1734	USA	392	397	53.1	59	0	4
2020-063A	PRCTEST SPACECRAFT	CHINA	331	347	50.2	0	1	5
2020-064A	GAOFEN 11 2	CHINA	236	595	97.3	0	1	0
2020-065A	JILIN-01 GAOFEN 3B	CHINA	528	547	97.5	8	1	0
2020-066A	HAIYANG 2C	CHINA	947	957	66.0	0	1	2
2020-067A	HJ-2A	CHINA	628	653	98.0	0	1	4
2020-067B	HJ-2B	CHINA	623	658	98.0			
2020-068A	GONETS M 17	RUSSIA	1476	1513	82.5	19	0	0
2020-068B	GONETS M 18	RUSSIA	1478	1511	82.5			
2020-068C	GONETS M 19	RUSSIA	1483	1506	82.5			
2020-069A	CYGNUS NG-14	USA	418	419	51.7	0	1	0
2020-070A	STARLINK-1644	USA	548	551	53.0	59	1	4
2020-071A	GAOFEN 13	CHINA	35777	35797	1.8	0	1	0
2020-072A	SOYUZ MS-17	RUSSIA	418	419	51.7	0	1	0
2020-073A	STARLINK-1819	USA	190	205	53.1	59	0	4
2020-074A	STARLINK-1847	USA	448	450	53.1	59	1	4
2020-075A	COSMOS 2547 (GLONASS)	RUSSIA	19114	19146	64.8	0	1	0
2020-076A	YAOGAN-30 U	CHINA	598	599	35.0	0	1	0
2020-076B	YAOGAN-30 V	CHINA	597	600	35.0			
2020-076C	YAOGAN-30 W	CHINA	594	603	35.0			
2020-076D	TIANQI-6	CHINA	584	603	35.0			
2020-077A	FLOCK 4 EP 1	USA	509	529	97.5	9	2	0
2020-078A	NAVSTAR 80 (USA 309)	USA	20181	20185	55.0	0	0	0
2020-079A	NUSAT-12 DOROTHY	ARGENTINA	465	480	97.3	13	1	0
2020-080A	TIANQI 11	CHINA	482	502	97.4	0	0	0
2020-081A	RISAT-2BR2	INDIA	569	576	36.9	9	1	0
2020-082A	TIANTONG-1 2	CHINA	35779	35796	5.4	0	1	0
2020-083A	USA 310	USA	NO INITIAL ELEMENTS			0	1	0
2020-084A	DRAGON RESILIENCE	USA	418	419	51.7	0	0	0
2020-085C	CORVUS BC5	USA	488	512	97.4	28	1	2
2020-086A	S6 MICHAEL FREILICH	ESA	1332	1344	66.1	0	1	0
2020-087A	CHANG'E 5	CHINA	LUNAR SAMPLE RETURN			0	0	0
2020-088A	STARLINK-1777	USA	379	381	53.1	59	0	4
2020-089A	LUCAS (JDRS-1)	JAPAN	35776	35799	0.0	0	1	0

\* Intl. = International; SC = Spacecraft; Alt. = Altitude; Incli. = Inclination; Addnl. = Additional; R/B = Rocket Bodies; Cat. = Cataloged

Notes:

1. Orbital elements are as of data cut-off date 03 Jan.

2. Additional spacecraft on a single launch may have different orbital elements.



National Aeronautics and Space Administration  
**Lyndon B. Johnson Space Center**  
2101 NASA Parkway  
Houston, TX 77058

[www.nasa.gov](http://www.nasa.gov)

<https://orbitaldebris.jsc.nasa.gov/>

The NASA Orbital Debris Photo Gallery has added high resolution, computer-generated images of objects in Earth orbit that are currently being tracked. They may be downloaded. Full instructions are at the webpage:

<https://orbitaldebris.jsc.nasa.gov/photo-gallery/>